Effect of heat treatment temperature on microstructure evolution of aluminum silicon coating on hot-formed steel

Zhen Wang[1], Rui Ge[2,†], Huan Xiao[2] and Yibin Sun[2]

[1]*Analytical and Testing Center, Wuhan University of Science and Technology, Wuhan 430081, China*

[2]*Faculty of Materials, Wuhan University of Science and Technology, Wuhan 430081, China*

[†]*E-mail: gerui@wust.edu.cn*

The present study delves into the influence of heat treatment temperature on microstructural and mechanical properties of aluminum silicon coatings applied to hot-formed steel substrates. Utilizing scanning electron microscopy (SEM), energy dispersive spectroscopy (EDS), and microhardness testing, a comprehensive analysis was conducted. Additionally, the phase composition of the aluminum-silicon coatings at varying heat treatment temperatures was elucidated using Facts age software. The findings indicate that the heat treatment temperature significantly impacts the diffusion of Fe, Al, and Si elements within the coating, leading to an increase in the thickness of the diffusion layer in the substrate as the temperature rises. Notably, the distribution of silicon-rich layers in the coating shifts towards the surface with increasing temperature, and the decrease in the proportion of silicon atoms results in a phase transformation from the single-phase $FeSiAl_2$ to a polyphase composition of $Al_{13}Fe_4$, Fe_2SiAl_2, and Al_5Fe_2. After heat treatment, the original austenite grains and martensitic laths undergo refinement, whereas the Vickers hardness of the substrate initially increases and subsequently decreases due to carbide precipitation. Consequently, considering the effects on diffusion layer thickness and matrix hardness, a heat treatment temperature of 950°C is deemed optimal.

Key words: Hot formed steel; Heat treatment temperature; Aluminum silicon coating; Microstructure evolution; Component distribution.

1. Introduction

Ultra-high strength steel has emerged as a pivotal material in the automotive sector, owing to its dual ability to enhance both vehicle safety and fuel economy. This trend is widely acknowledged and has been identified as a mainstream development in automotive materials [1]. Consequently, the demand for ultra-high strength steel in the automotive industry has witnessed a significant surge in recent years. However, despite its numerous advantages, the material is susceptible to challenges such as shape distortion, high forming loads, and substantial rebound during cold processing, thereby impeding its optimal utilization [2]. To address these issues, a novel thermal forming technology has been gradually gaining traction. Specifically, hot forming technology involves heating the hot stamping steel to a temperature range of 850°C to 950°C, maintaining this temperature for 3 min to 10 min to achieve a uniform austenitic structure. Subsequently, the steel is rapidly transferred to a mold equipped with a cooling system for stamping and forming. The rapid cooling process in the mold facilitates the transformation of austenite into martensite,

Y. Zhang and M. Ma (eds.), *Proceedings of the 7th International Conference on Advanced High Strength Steel and Press Hardening (ICHSU 2024)*, Atlantis Highlights in Materials Science and Technology 3,
https://doi.org/10.2991/978-94-6463-581-2_51

thereby substantially enhancing the material's strength [3]. The hot forming technology effectively mitigates the challenges associated with cold forming, including excessive rebound, forming difficulties, and cracking. The tensile strength of hot-formed parts can attain a remarkable value of 1500 MPa, thus enabling their widespread application in the automotive industry. Components such as B-pillars, door anti-collision beams, roof reinforcement beams, and chassis connectors are now routinely produced using this technology [4].

In the process of hot forming, the absence of coatings on traditional hot-stamping steel leads to decarburization and oxidation of the steel plate surface upon heating. This decarburization diminishes the surface strength of the steel, while the oxide layer elevates the friction coefficient between the steel plate and mold, thereby shortening the mold's service life and compromising subsequent coating performance. Consequently, it becomes imperative to eliminate the surface oxide through timed shot peening or pickling treatments, albeit these procedures escalate production costs and considerably impede production efficiency. Furthermore, shot peening introduces microcracks on the stamped part surface, ultimately deteriorating the service quality of the stamped parts [5]. To circumvent oxidation and decarburization and impart resistance to high-temperature oxidation and corrosion, Al-Si and hot-dip galvanized coatings are now predominantly utilized on hot-stamping steel plates [6].

The Al-Si coating, comprising a eutectic alloy with 10wt% Si, is the most prevalent choice for thermal forming steel coatings. This coating exhibits remarkable corrosion resistance and high-temperature oxidation resistance, effectively guarding against oxidation and decarburization of the steel plate's surface. Moreover, the steel plate's surface after hot forming maintains superb coating performance and corrosion resistance, making it particularly suited for high-temperature environments [7]. The present study delves into the impact of varying heating temperatures on the microstructure of the Al-Si coating and the matrix during hot stamping, aiming to contribute to the development of optimized heat treatment techniques for hot forming steel.

2. Materials and methods

The test material utilized in this study is an al-si coated hot-formed steel produced by a specific company. The base material is 27MnB5, possessing a thickness of 1.5 mm, and its chemical composition is detailed in Table 1. The industrial production of this Al-Si coated steel plate involves a continuous hot dip plating process. Post-pickling and other necessary treatments, the steel plate is transferred to a reduction furnace where it undergoes annealing at temperatures ranging from 800°C to 850°C. During this phase, a hydrogen-rich atmosphere is maintained to minimize oxide formation on the steel plate's surface. Subsequently, the steel plate is immersed in an aluminum liquid maintained at temperatures between 650°C and 750°C for the purpose of dipping and plating. The aluminum liquid is supplemented with 8% to 11% Si and 2% to 4% Fe, and the dipping duration is approximately 5 seconds. The resulting coating possesses a total weight of 150.0 g/m^2, a

thickness ranging from 19μm to 30μm, and a melting point of the Al-Si alloy between 580°C and 600°C.

Table 1 Chemical composition of 27MnB5 steel (wt%)

C	Mn	Si	B	Nb	Ti	Cr	P	S
0.27	1.20	0.25	0.003	0.02	0.02	≤0.35	≤0.025	≤0.005

The material was subjected to varying heating temperatures of 850°C, 900°C, 950°C, and 1000°C in a heating furnace, with a holding time of 5 minutes to induce austenitization of the sample. Following this, the austenitic sample was rapidly quenched in water to transform the austenite phase into martensite within the matrix, mirroring the heat treatment procedure in the hot stamping process. The steel plate was then sectioned into 10 mm × 10 mm specimens, and following cross-sectional inlaying, polishing, and further refinement, the microstructure and morphology of the Al-Si coating post-heat treatment were observed using a ThermoFisher Apreo S HiVac scanning electron microscope (SEM). The coating and diffusion layer thicknesses of each sample group were precisely measured using the electron microscope's scale. The coating composition was analyzed using an Oxford Ultim Max 100 EDS spectrometer. The Vickers hardness of the polished cross-sectional matrix was evaluated using an HV-1000B microhardness tester, with a test loading force of 300g and a pressure holding time of 10s. Additionally, the Fe-Si-Al ternary isothermal phase diagram at various heat treatment temperatures was simulated using Factsage software to gain further insights into the material's thermal behavior.

3. Results and discussion

3.1. *Microstructure of the original coating and matrix steel*

Figure 1 depicts the microstructural and compositional distribution of the pristine Al-Si coating. As evident from the figure 1, the original Al-Si coating comprises two distinct layers with a cumulative thickness of approximately 23μm. Notably, the outer layer is composed of an Al-Si eutectic phase. Furthermore, an Al-Si-Fe alloy diffusion layer of about 3μm thickness is discernible between the coating and the underlying steel matrix. Prior to hot forming, the steel matrix exhibits a spheroidized pearlite microstructure, as illustrated in Figure 2.

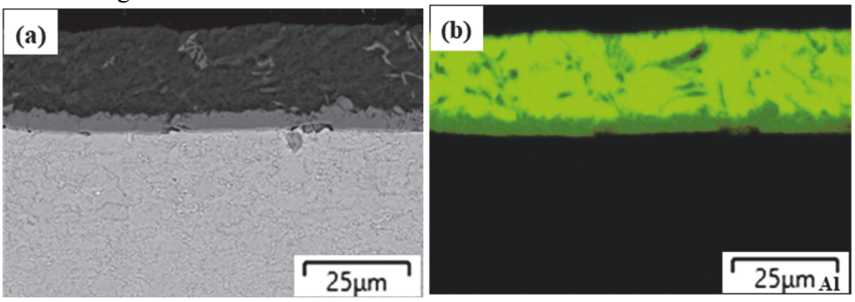

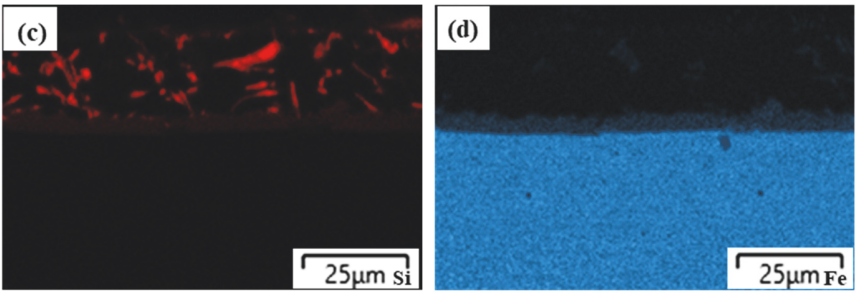

Fig.1 Original microstructure (a) and composition distribution of Al-Si coating(b) Al; (c) Si; (d) Fe

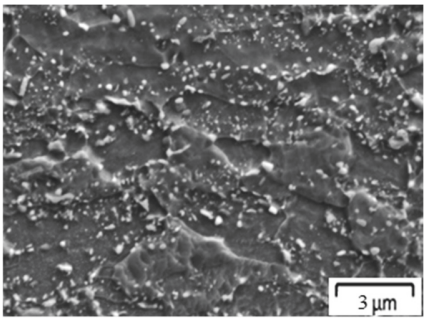

Fig.2 Matrix structure of hot formed steel before heat treatment

3.2. *Effect of heat treatment temperature on thickness and composition distribution of coating*

As depicted in Figure 3, variations in heating temperatures lead to alterations in the thickness of the coating and diffusion layer. With an increase in heat treatment temperature, there is a notable change in the element distribution within the coating, accompanied by a significant rise in the thickness of the diffusion layer. According to the Usibor1500P material standard provided by a company, specific requirements are formulated for the coating and diffusion layer thicknesses post-hot forming, stipulating that the coating thickness should be less than 50μm and the diffusion layer thickness should not exceed 16μm. Therefore, when the temperature reaches 1000°C, the diffusion layer thickness exceeds the specified limit, attaining 30μm, which elevates the coating's resistivity and could potentially compromise subsequent welding and coating performance. Conversely, at 850°C, the diffusion layer is excessively thin, measuring only 3μm, rendering it challenging to mitigate crack propagation during the hot forming process. This can lead to cracking and coating detachment. While cracks within the coating are typically attributed to the differential thermal expansion coefficients between brittle intermetallic compounds and the substrate during thermal cycling, it is noteworthy that few cracks propagate below the diffusion layer due to its excellent plasticity, which effectively impedes crack expansion [8-9].

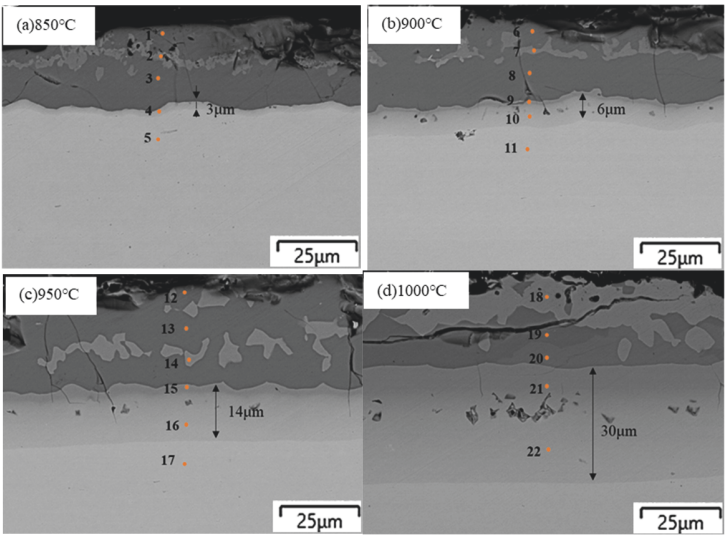

Fig.3 Changes of coating morphology and thickness at different heat treatment temperatures

Table2 presents the composition of Al, Fe, and Si elements within the Al-Si coating. The primary factor influencing the heat treatment process is the mutual diffusion of Fe and Al. Specifically, Al atoms diffuse from the coating surface towards the interior of the matrix, contributing to an augmentation in the thickness of the diffusion layer. Conversely, Fe atoms migrate from the matrix interior towards the coating surface. As the heat treatment temperature rises, the diffusion rate intensifies, leading to a substantial increase in the Fe content on the coating surface. The reciprocal diffusion of Fe and Al elements results in a reduction of these elements in the surface layer of the coating, thereby enhancing the proportion of silicon elements. Additionally, with an increase in heat treatment temperature, the distribution area of the silicon-rich zone gradually shifts from the coating's middle towards its surface. Furthermore, the Si content within this silicon-rich zone decreases as a consequence of the diffusion process during heat treatment.

Table 2 Distribution of main elements in sample coating

Sample		Al	Si	Fe	at. %	Sample		Al	Si	Fe	at. %
850℃	1	68.7	5.0	26.3	Fe:Al 2:5, little Si	**1000℃**	18	46.7	6.7	46.6	Fe: Si: Al 7:1:7
	2	50.5	15.9	33.6	Fe: Si: Al 2:1:3		19	68.6	1.4	30.0	Fe:Al 1:2, little Si
	3	67.6	3.4	29.0	Fe:Al 2:5, little Si		20	64.4	1.4	34.2	Fe:Al 1:2, little Si
	4	22.2	4.8	72.9	Fe:Al 3:1, little Si		21	46.0	6.2	47.7	Fe: Si: Al 7:1:7
	5	0	0.7	99.3	Fe, little Si		22	15.3	3.5	81.2	Fe:Al 5:1, little Si

900℃	6	70.9	3.9	25.2	Fe:Al 2:5，little Si	950℃	12	69.0	2.5	28.5	Fe:Al 1:3，little Si
	7	49.0	16.3	34.7	Fe: Si: Al 2:1:3		13	67.6	2.2	30.2	Fe:Al 1:3，little Si
	8	67.0	3.3	29.7	Fe:Al 2:5，little Si		14	42.2	11.1	46.7	Fe: Si: Al 4:1:4
	9	39.1	13.9	47.0	Fe: Si: Al 7:2:5		15	41.4	10.8	47.8	Fe: Si: Al 5:1:4
	10	14.5	3.4	82.1	Fe:Al 11:2，little Si		16	17.1	6.1	76.8	Fe: Si: Al 12:1:3
	11	0	0.7	99.3	Fe，little Si		17	0	0.6	99.4	Fe，little Si

During the heat treatment process, when the heating temperature surpasses the melting point of aluminum, the coating transitions into a liquid state, analogous to the dipping plating process. This initiates the reaction-diffusion between Fe and Al, culminating in the formation of intermetallic compounds. The diffusion coefficient of the elements varies with temperature, adhering to the Arrhenius equation $D=D_0\exp(-Q/RT)$, where D_0 represents a constant influenced by the concentration of the diffusing species, Q denotes the activation energy of the diffusion process, R is the gas constant, and T stands for the absolute temperature. Consequently, the diffusion rates of Al and Fe are influenced by the quenching temperature, leading to variations in the distribution concentrations of aluminum, silicon, and iron within the coating during identical quenching durations, as evident in Table 1.

Figure 4 depicts the Fe-Si-Al ternary phase diagram at various heat treatment temperatures, analyzed using Factsage software. At a heat treatment temperature of 850°C, the composition of the bright silicon-rich phase of the coating reveals an Al content of 50.48 at%, 15.94 at% Si, and 33.58 at% Fe, primarily comprising $FeSiAl_2$. The dark aluminum phase has an approximate Al content of 68 at%, with Fe ranging between 26 at% and 20 at%, corresponding to $Al_{13}Fe_4$. The diffusion layer exhibits a low Al content. The inner layer primarily consists of bcc-Fe, characterized by a high Fe content. As the temperature increases, a more significant variation in the proportion of Fe, Si, and Al in the Si-rich layer is observed, as indicated in Table 1. Specifically, when the quenching temperature reaches 900°C, an additional Si-rich layer emerges between the coating and the diffusion layer. Based on the proportions of Fe, Si, and Al elements, the primary composition of this layer is $Al_{13}Fe_4 + Fe_2SiAl_2$. As the temperature escalates to 950°C, the proportion of Fe and Al in the silicon-rich layer undergoes further changes, maintaining a primary composition of $Al_{13}Fe_4 + Fe_2SiAl_2$. At a quenching temperature of 1000°C, the Si content in the Si-rich layer diminishes to 6 at%, with the main component phases being $Al_{13}Fe_4 + Fe_2SiAl_2 + Al_5Fe_2$.

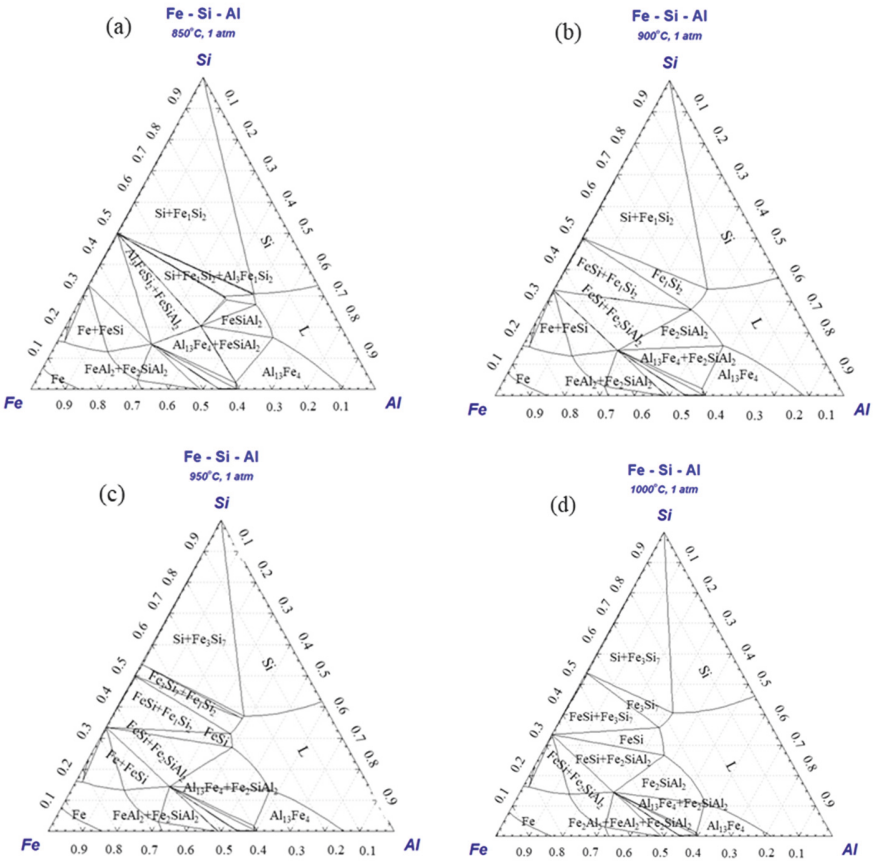

Fig.4 Fe-Si-Al ternary phase diagram at different heat treatment temperatures

3.3. *Effect of heat treatment temperature on structure and hardness of matrix*

Figure 5 illustrates the microstructural transformations in the matrix of hot-formed steel subjected to varying heat treatment temperatures. When the heat treatment temperature ranges from 850°C to 1000°C, the matrix undergoes complete austenitization, resulting in the formation of acicular martensite following water-cooled quenching. Notably, as the quenching temperature increases, the size of the acicular martensite gradually decreases. Figure 6 depicts the evolution of primary austenite grains in the matrix of hot-formed steel at different heat treatment temperatures. As the quenching temperature rises, a discernible reduction in the average size of the primary austenite grains within the matrix is observed. Table3 summarizes the Vickers hardness values of the matrix at various quenching temperatures. It is evident that the hardness of the matrix increases progressively with an increase in quenching temperature. However, a notable exception is observed at a quenching temperature of 1000°C, where the hardness of the matrix undergoes a decrease.

As the quenching temperature escalates, two concurrent phenomena occur, which ultimately shape the hardness profile of the steel matrix. Firstly, the martensitic strip exhibits a refinement trend, while the average size of the original austenite grain undergoes a substantial decrease from 11μm at 850°C to 5μm at 950°C. This refinement contributes significantly to an increase in the structural hardness. However, when the quenching temperature further rises to 1000°C, the average austenite grain size remains relatively unchanged compared to 950°C. Secondly, during the quenching process, carbide precipitation occurs within the matrix. This carbide is soluble in the austenite matrix and, upon quenching, the carbon supersaturation transforms into martensite. The carbon content is a pivotal factor influencing the hardness [10]. At a quenching temperature of 850°C, carbide primarily precipitates at the grain boundaries. With increasing quenching temperature, the amount of carbide precipitation within the grains also increases, particularly evident at 1000°C. This carbide precipitation notably diminishes the hardness of the martensite. Consequently, the combined effect of these two factors results in a hardness profile where the matrix of the hot-quenched steel initially experiences an increase in hardness, followed by a decrease, as the quenching temperature rises.

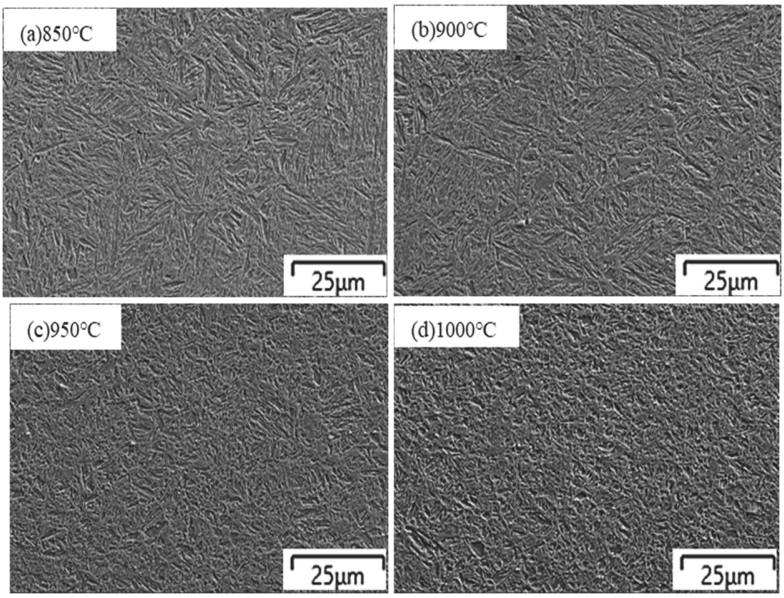

Fig.5 Microstructure of thermoformed steel matrix at different heat treatment temperatures

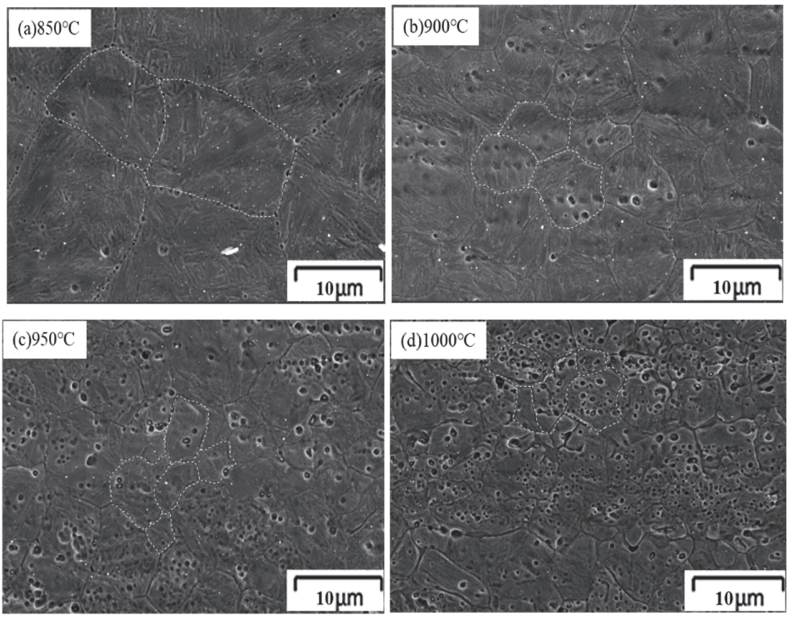

Fig.6 Austenitic grain boundary diagram of thermoformed steel matrix at different heat treatment temperatures

Table 3 Microhardness of matrix at different quenching temperatures ($HV_{0.3}$)

Sample	1	2	3	Average value
850°C	697	709	703	703
900°C	735	709	716	720
950°C	742	770	749	753
1000°C	703	709	716	709

4. Conclusion

As the heat treatment temperature escalates, the Al element undergoes diffusion from the coating into the substrate, while the Fe element diffuses in the opposite direction, from the substrate towards the coating. Consequently, this bidirectional diffusion process leads to a notable increase in the thickness of the diffusion layer within the coating. Additionally, the proportion of silicon atoms within the silicon-rich layer diminishes, and these atoms gradually redistribute towards the surface of the coating. Furthermore, the compositional phase of the silicon-rich layer undergoes a transformation, shifting from a sole $FeSiA_{12}$ phase to a mixture comprising $Al_{13}Fe_4$, Fe_2SiA_{12}, and Al_5Fe_2.

Following heat treatment, the microstructure of the thermoformed steel matrix undergoes a distinct transition, transforming from spheroidized pearlite to acicular martensite. As the heat treatment temperature rises, the original austenite grain size diminishes, and the martensitic lath becomes notably refined. However, concurrently, the amount of carbide precipitation within the matrix also augments. This complex interplay

of phenomena leads to a biphasic trend in the Vickers hardness of the matrix, initially increasing and subsequently decreasing.

Upon comprehensive consideration of the diffusion layer thickness and matrix strength, it is determined that the optimal thermoforming temperature is 950℃. At this temperature, the diffusion layer thickness attains a value of 14μm, while the Vickers hardness of the matrix is recorded as $753HV_{0.3}$.

Acknowledgement

This work is supported by China National Science Foundation (U20A20270).

References

1. Yasutaka S，Kenichiro M，Tomoyoshi M，et a1. Improvement of formability using partial cooling during transfer in hot stamping of ultra-high strength steel parts. Procedia Manufacturing，2018，15(3)：1119-1126.
2. Zhu P，Hu T H，Wu T H，et a1. Progress in welding techniques for hot stamped ultra-high strength steel. Shanghai Metals，2023，45(3)：1-12.
3. Wei Y S. 22MnB5 press forming process and application technology. Hebei Metallurgy，2023，(10)：50-54.
4. Tang Q，Gua P C，Luo hong，et a1. Hot deformation Behavior and hot processing map of hot-formed 22MnB5 ultra-high strength steel for automobile body. Materials Reports，2023，37(18)：206-212.
5. Li Q K，Liu Q B， Sun X Q，et a1. Influence of process parameters of hot stamping to microstructure and mechanical properties of ultra high strength hot-formed steel. Heat Treatment Technology and Equipment，2023，44(3)：9-11.
6. Zhang J，Jiang S M，Zhang Q F. Current status of coating for hot formed steel. Heat Treatment of Metals，2015，(3)：169-172.
7. Lü J S，Xu W H，Yang H G，et a1. Effect of holding temperature of hot stamping on microstructure of Al-Si coating of 22MnB5 steel. Steel Rolling，2024，41(2)：92-96.
8. Pelcastre L，Hardell J，Rolland A，et al. Influence of microstructural evolution of Al-Si coated UHSS on its tribological behavior against tool steel at elevated temperatures. Journal of Materials Processing Technology，2015，228：117-124.
9. Gui Z X，Liang W K，Zhang Y S，et a1. Enhancing ductility of the Al-Si coating on hot stamping steel by controlling the Fe-A1 phase transformation during austenitization. Technological sciences. 2014(57)：1785-1793.
10. Hande G，Ertan R，Zcan R. Influence of Heat Treatment Parameters on the Microstructure and Mechanical Properties of Boron-Alloyed Steels. Materials Testing，2003，54(9)：619-624.